

# Direct Measurements of Nonlinear Absorption and Refraction in Solutions of Phthalocyanines

T. H. Wei<sup>1</sup>, D. J. Hagan<sup>1</sup>, M. J. Sence<sup>1</sup>, E. W. Van Stryland<sup>1</sup>, J. W. Perry<sup>2</sup>, and D. R. Coulter<sup>2</sup>

<sup>1</sup> Center for Research in Electro-Optics and Lasers and Department of Physics, University of Central Florida, Orlando, FL 32816, USA

<sup>2</sup> Jet Propulsion Laboratory, California Institute of Technology, Pasadena, CA 91109, USA

Received 16 June 1991/Accepted 12 September 1991

**Abstract.** We report direct measurements of the excited singlet state absorption cross section and the associated nonlinear refractive cross section using picosecond pulses at 532 nm in solutions of phthalocyanine and naphthalocyanine dyes. By monitoring the transmittance and far field spatial beam distortion for different pulsewidths in the picosecond regime, we determine that both the nonlinear absorption and refraction are fluence (energy per unit area) rather than irradiance dependent. Thus, excited state absorption (ESA) is the dominant nonlinear absorption process, and the observed nonlinear refraction is also due to real population excitation.

**PACS:** 33.00, 42.65, 42.80

In recent years, conjugated organic molecules and polymers have come under critical study regarding their potential as nonlinear optical materials [1]. This has led to interest in: 1) developing a fundamental understanding of the mechanisms which contribute to the nonlinear optical response, 2) identifying means of enhancing and maximizing the nonlinear susceptibilities, and 3) obtaining well defined and accurate measurements of the refractive and absorptive contributions to the observed nonlinearities. Here we report on the separation of nonlinear absorption and refraction in phthalocyanine and naphthalocyanine solutions on the picosecond timescale using a combined nonlinear transmittance and beam distortion method which we refer to as the “Z-scan” technique [2, 3]. We find that both the nonlinear absorption and refraction are dominated by creation of a real population of excited states even though the wavelength of observation lies between electronic absorption bands.

Metallophthalocyanines and related conjugated ring molecules have attracted recent interest [4–11] because, as confined, reduced-dimensionality (2D) delocalized electronic systems, large electronic nonlinearities are expected. The rigid structural framework of these molecules leads to a small geometry change on excitation and a concentration of intensity into the  $S_1 \leftarrow S_0$  0,0 vibronic transition, resulting in a strong narrowband absorption ( $Q(0)$  band) [12]. Thus, the phthalocyanine dyes can exhibit a low saturation intensity depending on the relevant relaxation rates. For example, chloro-aluminium phthalocyanine (CAP) is well known as a saturable absorber at

694 nm and was used early on as a passive  $Q$ -switch for ruby lasers [13–15]. It also exhibits excited triplet state absorption [16] at shorter wavelengths in the range between the  $Q$  and  $B$  bands [12] where the linear absorption is quite weak. The nonlinear optical response in this spectral region is of interest because it can function as an optical pulse energy limiter [6, 11]. This type of response has been referred to as reverse saturable absorption [17].

As part of our search for dyes which may be useful for optical limiting applications, we have surveyed the nonlinear transmission of a number of metallophthalocyanines and metallo-naphthalocyanines [6, 11]. Here, we present data using picosecond laser pulses on two dyes in solution: CAP in methanol solution and a silicon naphthalocyanine (Nc) derivative [18],  $\text{Si}(\text{OSi}(n\text{-hexyl})_3)_2\text{Nc}$ , which we will refer to as SINC, in toluene solution. The  $Q$ -band absorption peaks of these solutions are at 670 nm and 774 nm respectively, while we are exciting at 532 nm. With picosecond input pulses (shorter than the time required to populate the triplet state), we find that the excited singlet state absorption is quite strong for both dyes [6, 11]. The generic level structure for these molecules is shown in Fig. 1, and consists of five levels showing the possibility of both excited singlet and excited triplet state absorption. The linear absorption at 532 nm is initially low since we are exciting high in the vibrational manifold of  $S_1$ . The fast relaxation to the bottom of this electronic state makes the excited state absorption (ESA) resonant with the 532 nm input light. For longer pulses, intersystem crossing also leads to resonant triplet

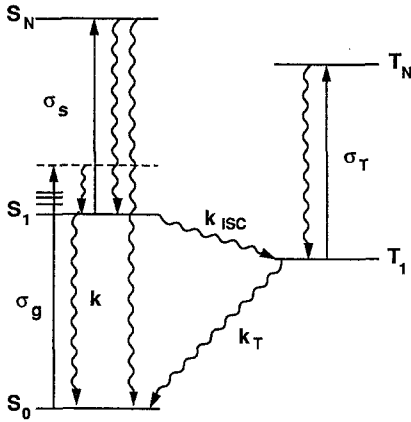


Fig. 1. Generic five-state model for nonlinear behavior of phthalocyanines.  $S_0$ ,  $S_1$ , and  $S_N$  are singlet states and  $T_1$  and  $T_N$  are triplet states. The  $\sigma$ 's are absorption cross sections and the  $k$ 's are rate constants.  $\sigma_s$  is represented in the text simply as  $\sigma$ . Wavy lines correspond to spontaneous decay processes. The total decay rate constant for  $S_1$  is  $k_S = k + k_{ISC}$

state ESA. This ability to respond on both fast and slow timescales makes these materials particularly attractive for optical limiting. The singlet lifetimes and triplet state formation yields for both CAP and SINC are listed in Table 1.

## 1 Excited State Absorption

In the following analysis we examine the nonlinear transmittance of a material in which ESA is dominant. In Sect. 3 we show this to be the case for these materials. We solve a rate equation model including excited singlet-singlet state absorption as well as integration over the transverse beam profile. In this model we ignore saturation as discussed in Sect. 4. For pulses short relative to the decay time of the intermediate level the following equations apply:

$$dI/dz' = -\alpha I - \sigma N I \quad (1)$$

and

$$dN/dt = \alpha I / \hbar \omega, \quad (2)$$

where  $dz'$  is the differential element of depth in the sample,  $I$  the irradiance,  $\alpha$  the linear absorption coefficient,  $\sigma$  the excited singlet-singlet absorption cross section,  $N$  the density of excited states, and  $\hbar\omega$  the photon energy. By temporal integration of (1) and (2) we find

$$dF/dz' = -\alpha F - \alpha \sigma / 2 \hbar \omega F^2, \quad (3)$$

where  $F$  is the fluence (i.e. energy per unit area). The solution to this equation, after integrating over the Gaussian spatial distribution of the pulse of on axis fluence  $F_0$ , gives the normalized change in transmittance  $\Delta T$  of

$$\Delta T = \frac{T}{T_{lin}} - 1 = \frac{\ln(1+q)}{q} - 1 \cong -\frac{q}{2} = -\frac{\alpha \sigma F_0 L_{eff}}{4 \hbar \omega}, \quad (4)$$

where  $T$  is the transmittance,  $T_{lin}$  the linear transmittance, and  $L_{eff} = (1 - e^{-\alpha L})/\alpha$  with  $L$  the sample length. Here the last equality defines  $q$  and the approximation is valid for small  $q$  (i.e. for small  $\Delta T$ ). All energy and fluence levels are quoted as incident in the fluid (i.e. after surface reflections are taken into account).

From (4), the same  $F$  for two different pulsewidths is expected to give the same nonlinear absorption for ESA. A similar analysis for two-photon absorption (2PA) gives a result that is  $I$  rather than  $F$  dependent. Thus, the transmittance change  $\Delta T$  at a fixed input pulse energy will be independent of pulsewidth for ESA, but will depend on pulsewidth for 2PA. This serves as a simple test to determine the nonlinear mechanism.

## 2 Z-Scan Techniques

Most of the measurements of the nonlinear properties reported in this paper employed the "Z-scan" technique. This technique, as shown in Fig. 2, involves measurements of the far field sample transmittance of a focused Gaussian beam as a function of the position ( $Z$ ) of the material relative to the beam waist [2, 3]. Here, we give a brief description of the determination of nonlinear absorption and refraction using this method. First, consider a sample with a negative nonlinear refractive index and an aperture in place in Fig. 2. If we normalize the transmittance  $T$  to the linear transmittance of the aperture, and we begin the scan at large negative values of  $Z$  in Fig. 2,  $T$  is unity. As the sample is moved toward the focus of a

Table 1. Singlet and triplet properties of CAP and SINC

Molecule	$\tau_S^a$	$\phi_T^b$	$\tau_{ISC}^c$	$\epsilon_g^d$	$\epsilon_T^e$	$\epsilon_S^f$
CAP <sup>g</sup>	7.0 (1)	0.4 <sup>h</sup>	18	580 (40)	19,000	6,000
SINC <sup>i</sup>	3.15 (5)	0.2 <sup>j</sup>	16	740 (40)	40,000	10,200

<sup>a</sup>  $S_1$  fluorescence lifetime (ns) measured using time-correlated single photon counting

<sup>b</sup> Triplet yield

<sup>c</sup> Calculated intersystem crossing time constant (ns)

<sup>d</sup> Ground state extinction coefficient ( $M^{-1} cm^{-1}$ ) at 532 nm

<sup>e</sup> Triplet-triplet extinction coefficient ( $M^{-1} cm^{-1}$ ) at 532 nm estimated from  $T-T$  spectra in [16] for CAP and [20] for SINC

<sup>f</sup> Excited singlet-singlet extinction coefficient ( $M^{-1} cm^{-1}$ ) calculated from measured  $\sigma$  values, this work

<sup>g</sup> In ethanol solution

<sup>h</sup> In 1-chloronaphthalene solution, [19]

<sup>i</sup> In toluene solution

<sup>j</sup> [20]

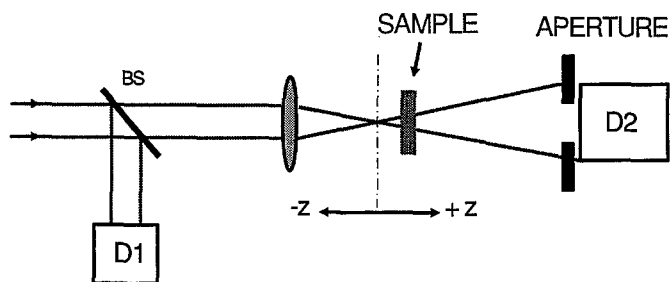


Fig. 2. The Z-scan experimental apparatus in which the ratio  $D2/D1$  is recorded as a function of the sample position  $Z$

laser beam the increased irradiance leads to a negative lensing effect which tends to collimate the beam, thus increasing the energy transmitted through the aperture ( $T > 1$ ). With the sample on the  $+Z$  side of focus, the negative lensing effect tends to augment beam divergence and the energy transmittance is reduced ( $T < 1$ ). The approximate null at  $Z \cong 0$  is analogous to the effect of placing a thin lens at focus which results in a minimal far field pattern change. For still larger  $+Z$  values the irradiance is reduced and the transmittance returns to unity. A positive nonlinearity results in the opposite effect, i.e. lowered transmittance for the sample at negative  $Z$  and enhanced transmittance for positive  $Z$ . The Z-scans are readily analyzed to extract the nonlinear refraction as described in detail in [3].

The induced peak-on-axis phase distortion  $\Delta\Phi_0$  is determined by integration of the following equation through the entire length  $L$  of the sample:

$$d\Phi_0/dz' = 2\pi\Delta n(z')/\lambda, \quad (5)$$

where  $\Delta n$  is the irradiance or fluence dependent change in refractive index and  $\lambda$  is the wavelength.  $z'$  is the distance within the sample, to be distinguished from the sample position,  $Z$ . For an instantaneous (irradiance dependent) nonlinearity  $\Delta n = n_2|E|^2/2$ , where  $|E|$  is the electric field amplitude. For an index change due to population of an excited state,

$$\Delta n = \frac{\sigma_r N \lambda}{2\pi}, \quad (6)$$

where  $\sigma_r$  is defined as the nonlinear refractive cross section. Thus, from (2)  $\Delta n$  depends on the temporal integral of the irradiance, or more simply, the fluence.

If the aperture in the Z-scan experiment of Fig. 2 is removed (we term this an "open" aperture Z-scan as opposed to "closed" aperture described above), the Z-scan becomes insensitive to nonlinear refraction and results in a null signal (i.e. flat response with  $Z$ ) unless nonlinear absorption is present. In this case a symmetrical curve showing a reduced transmittance ( $T < 1$ ) about the focal position is obtained described by (4) where  $F_0$  is a function of  $Z$ . If both nonlinear refraction and nonlinear absorption are present simultaneously, an analysis of the open and closed aperture Z-scans can be used to separately determine the nonlinear refraction and nonlinear absorption.

The separation and evaluation process is simple: the closed aperture normalized Z-scan is divided by the one with the aperture open. The result is a new Z-scan showing the sign and magnitude of the refractive nonlinearity. This division process will give a faithful representation of the nonlinear refraction as if nonlinear absorption were absent for relatively small nonlinear absorption. However, in the case of the large ESA shown by these dyes nonlinear absorption dominates, and we fit the data by numerical solution of (2-6) following the analysis given in [3].

### 3 Experiment and Results

CAP (Eastman Kodak Co.), was extracted from the commercial product with methanol and filtered to remove insoluble material. The methanol was removed by rotary evaporation using a room temperature bath. The resulting solid CAP was used for experiments. SINC was synthesized by the method described in [18]. Solvents used for measurements were absolute methanol for CAP and high purity toluene for SINC.

In our experiments, we use single pulses of picosecond duration at 532 nm with a high quality TEM<sub>00</sub> spatial mode obtained from a frequency doubled mode-locked Nd:YAG laser, with a single pulse switch-out apparatus. By selection of various etalons within the laser cavity, the pulsewidth can be varied from 30 to 100 ps full width at half maximum (FWHM). For all of our Z-scan measurements, the beam is focused to a waist of radius  $w_0 = 19 \mu\text{m}$  half width at  $1/e^2$  maximum (HW1/e<sup>2</sup>M) and the sample path length is 1 mm.

We performed Z-scan experiments on CAP at a concentration of  $1.3 \times 10^{-3}$  moles per liter. The linear transmittance of 84% gives a linear absorption coefficient of  $\alpha = 1.8 \pm 0.1 \text{ cm}^{-1}$ , which corresponds to an extinction coefficient of  $580 \pm 40 \text{ liters cm}^{-1} \text{ mole}^{-1}$ . Here the extinction coefficient is defined as,  $\epsilon = -\log_{10} T/CL = 10^{-3}\sigma N_A/\ln(10)$ , where  $C$  is the concentration in moles per liter. We also give the relation for an absorption cross section  $\sigma$  in  $\text{cm}^2$  where  $N_A$  is Avogadro's number. In this paper we use  $\sigma$  as the ESA cross section. Similar measurements on SINC give a transmittance of 84% ( $\alpha = 1.8 \pm 0.1 \text{ cm}^{-1}$ ) at a concentration of  $1.0 \times 10^{-3}$  mole per liter, corresponding to an extinction coefficient of  $740 \pm 40 \text{ liters cm}^{-1} \text{ mole}^{-1}$ .

Figure 3 shows open aperture Z-scans on a CAP solution at 532 nm for two different pulsewidths of 29 ps and 61 ps (FWHM) using the same input energy of 1.17  $\mu\text{J}$  and hence, the same on axis fluence at focus of  $F_0(Z=0) = 205 \text{ mJ/cm}^2$ . Clearly the nonlinear transmittance is independent of pulsewidth and hence we conclude that the mechanism is dominated by ESA.

The solid lines in Fig. 3 are the results of numerically fitting the data to (4) by integrating over space. Here  $F_0$  is a function of  $Z$ . This numerical fit gives a value for  $\sigma$  of  $\cong 2.3 \times 10^{-17} \text{ cm}^2$  ( $\epsilon = 6,020 \text{ liters cm}^{-1} \text{ mole}^{-1}$ ). Measurements show that  $\sigma$  is the same for concentrations of  $5.5 \times 10^{-4}$  moles per liter and  $1.3 \times 10^{-3}$  moles per liter. A similar measurement on SINC gave  $\sigma$  of  $\cong 3.9 \times$

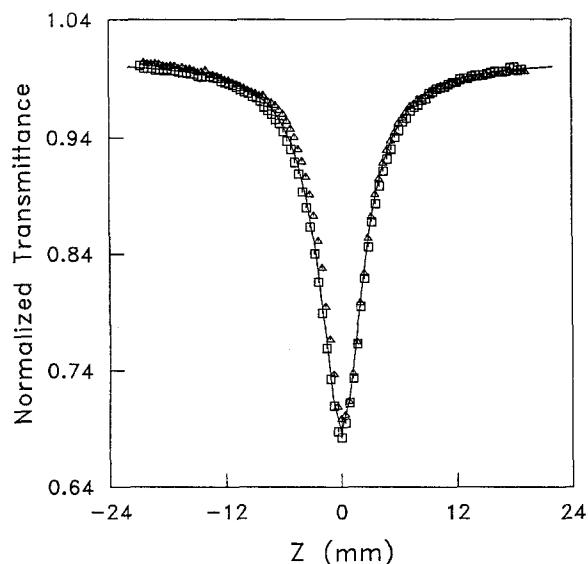


Fig. 3. Open aperture Z-scans for 29 ps (squares) and 61 ps (triangles) pulsewidths at an incident energy of  $1.16 \mu\text{J}$  in CAP

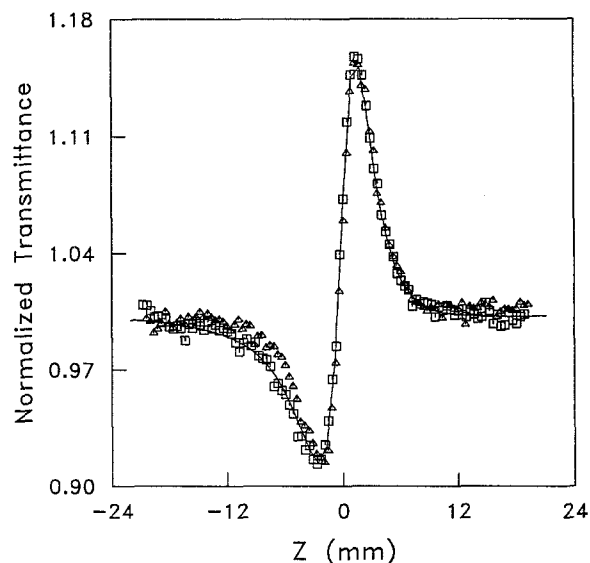


Fig. 4. The results of the division of the closed aperture Z-scan data by the open aperture Z-scan data of Fig. 3 for 29 ps (squares) and 61 ps (triangles) pulsewidths at an incident energy of  $1.16 \mu\text{J}$  in CAP

$10^{-17} \text{ cm}^2$  ( $\epsilon = 10,200 \text{ liters cm}^{-1} \text{ mole}^{-1}$ ). We obtain the same values for  $\sigma$  in CAP at input fluence from  $0.4 \mu\text{J}$  to  $3.6 \mu\text{J}$  and for SINC from  $0.4 \mu\text{J}$  to  $1.9 \mu\text{J}$ . Absolute errors in the  $\sigma$  values of  $\pm 13\%$  were determined from an estimated 7% error in the concentration, 5% fitting error and a 10% possible error in the fluence calculation.

In order to determine the nonlinear refractive coefficients of these dyes, we performed closed aperture Z-scans on CAP for 29 ps and 61 ps (FWHM) pulsewidths. Figure 4 shows the results of dividing these Z-scans by the open-aperture scans of Fig. 3 taken under identical conditions. Clearly we see that the index change is positive and identical for the same fluence. This nonlinear refraction is therefore fluence dependent and as-

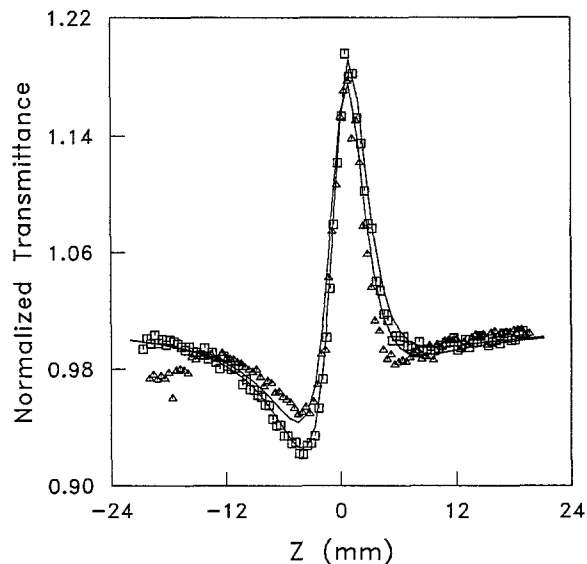


Fig. 5. The results of the division of the closed aperture Z-scan data by the open aperture Z-scan data for 29 ps (squares) and 61 ps (triangles) pulsewidths at an incident energy of  $1.89 \mu\text{J}$  in SINC

sociated with the real excitation of the singlet state. To determine the contribution of the solvent, Z-scans were performed on the pure methanol and toluene solvents. This yielded an  $n_2$  for methanol of  $2.5 \times 10^{-13} \text{ esu}$  and for toluene of  $1.9 \times 10^{-12} \text{ esu}$ . As expected, no nonlinear absorption was seen in the pure solvents. For the calculation of  $\sigma_r$ , contributions of both solvent ( $n_2$ ) and dye ( $\sigma_r$ ) were included, thus  $\Delta n = n_2|E|^2/2 + \sigma_r N \lambda / 2\pi$ . Substituting this expression into (5) and temporally integrating to numerically fit the data of Fig. 4 then yields  $\sigma_r = 1.8 \times 10^{-17} \text{ cm}^2$  for CAP. Measurements at concentrations of  $\cong 5.5 \times 10^{-4} \text{ moles/liter}$  and  $\cong 1.3 \times 10^{-3} \text{ moles/liter}$  in CAP showed the same  $\sigma_r$ . In Fig. 5, we show divided Z-scans for SINC, again for pulsewidths of 29 ps and 61 ps (FWHM) and with an incident energy of  $1.89 \mu\text{J}$ . The solid lines show fits, obtained in the same way as described above for CAP, giving  $\sigma_r = 4.7 \times 10^{-18} \text{ cm}^2$  for SINC. The reason that the two curves in Fig. 5 do not coincide, as do the curves for CAP, is that the instantaneous large nonlinear refraction ( $n_2$ ) of the toluene solvent plays a significant role. In the case of CAP, the overlap of the Z-scans at different pulsewidths and the independence of our measurements on concentration indicate that the nonlinear refractive contribution of the solvent is negligible. We obtain the same values of  $\sigma_r$  over the input fluence ranges quoted for the determination of  $\sigma$ .

#### 4 Discussion

Our results demonstrate the importance of measuring the nonlinearities at different pulsewidths. Had we looked with only a single pulsewidth, we could equally well have fit the data of Figs. 4 and 5 with simple  $n_2$  values. For example for a pulsewidth of 29 ps for CAP this gives an  $n_2 = 4.6 \times 10^{-12} \text{ esu}$  and for SINC this gives

$n_2 = 3.0 \times 10^{-12}$  esu. However, we would obtain a larger  $n_2$  using 61 ps. From these fits and the  $n_2$ 's of the solvents, the contribution to the "effective"  $n_2$ 's for CAP and SINC at the given concentrations can be obtained by simple subtraction to give  $n_2 = 4.4 \times 10^{-12}$  esu for CAP and  $n_2 = 1.1 \times 10^{-12}$  esu for SINC. These correspond to effective third order hyperpolarizabilities of  $4.5 \times 10^{-31}$  esu for CAP and  $3.3 \times 10^{-32}$  esu for SINC. The "effective"  $n_2$  is only globally valid if the index change is dependent on the instantaneous irradiance and hence responds on an ultrafast timescale. The most common example of this is the bound electronic Kerr effect. However, if it is due to the population of excited states, it is much more useful to quote the excited state refractive coefficient. Hence what we are observing is not a true  $\chi^{(3)}$  effect but is a sequential  $\chi^{(1)} : \chi^{(1)}$  process, where  $\chi^{(j)}$  refers to the  $j$ th order electric susceptibility. Here, the first  $\chi^{(1)}$  is associated with the ground state absorption, the second with the resulting excited state refraction.

These refractive changes are a direct result of the changes in the linear absorption, as described by the Kramers–Kronig relations [20]. These relations predict a decrease in index above the induced absorption resonance and an increase below resonance. We can speculate that the cause for the observed positive sign of the nonlinear refraction is the addition of such an absorption centered at a slightly shorter wavelength than our 532 nm light. Measurements of the transient absorption spectrum confirm increasing the absorption centered at a shorter wavelength than 532 nm for CAP [6]. In SINC it is not clear where with respect to 532 nm the increased absorption is centered, and we see a considerably smaller positive nonlinear refraction. In addition we are on the high frequency side of the  $Q$ -band absorption which we are saturating. The nonlinear refraction from this saturation is, therefore, also positive in both CAP and SINC.

We have ignored the above mentioned saturation of the  $Q$ -band absorption, i.e. depletion of the ground state population, since we experimentally do not see a significant deviation from the fits using (4) and (6) until nearly an order of magnitude higher input fluence. This is our observation even though a simple calculation shows significant ground state depletion at the fluence levels used in these experiments. Allowing for saturation in the rate equations, and numerically integrating, gives excited state cross sections nearly 30% larger than we quote. However, we find a much better fit to the data over the entire range of input fluences used in these experiments with the simple (nonsaturating) model given here. A partial direct repopulation of the ground state from the excited state absorption process may account for the absence of saturation. Time resolved absorption spectra would answer this question. Nevertheless, the main conclusion that excited state absorption and excited state refraction dominate in these experiments remains unchanged.

Garito et al. [9] have recently reported an enhancement of the third order hyperpolarizability using third harmonic generation at 1.54  $\mu\text{m}$  upon optically inducing a population in the excited singlet state. In our experiments this would appear as a higher order nonlinearity (i.e. a  $\chi^{(1)} : \chi^{(3)}$  process,  $\chi^{(1)}$  for the initial excitation to the ex-

cited state, and  $\chi^{(3)}$  for the subsequent increase in hyperpolarizability). Therefore, the excited state nonlinearities we observe are not directly related to the nonlinearities observed by Garito.

A summary of the results of our measurements along with the singlet and triplet photophysical properties of CAP and SINC are given in Table 1. The excited singlet lifetimes are two orders of magnitude longer than the 30–60 ps pulse durations used in our measurements, so that our results are for excited singlet absorption and we neglect singlet decay in the analysis. While the excited singlet extinction coefficients are roughly an order of magnitude larger than those for the ground states at this wavelength, they are a factor of 3 to 4 smaller than those for the triplet states at 532 nm. The triplet absorption would play a significant role only with much longer pulses.

## 5 Conclusion

In conclusion we have used a simple sensitive single beam technique ( $Z$ -scan) to measure both nonlinear absorption and nonlinear refraction in solutions of phthalocyanine and naphthalocyanine dyes on a picosecond time scale. The nonlinear refraction is determined to be positive and both the nonlinear absorption and refraction are dependent on input pulse fluence (i.e. depend on the excited singlet state population). We give simple relations that allow this excited state absorption cross section and the associated nonlinear refractive cross section to be obtained directly from  $Z$ -scan data. For longer nanosecond time scales the triplet excited state absorption becomes significant and will lead to further enhancement of the absorptance. These materials are, therefore, promising materials for optical limiting applications.

*Acknowledgements.* A portion of this work was performed by the Jet Propulsion Laboratory, California Institute of Technology, as part of its Center for Space Microelectronics Technology. This work was supported in part by the U.S. Army Vulnerability Assessment Laboratory (VAL, LABCOM) through an agreement with the National Aeronautic and Space Administration. The CREOL authors also gratefully acknowledge the support of the U.S. Army Research Office, VAL, LABCOM, the National Science Foundation grant # ECS-8617066, DARPA/CNVEO and the Florida High Technology and Industry Council. The authors also thank Prof. M. E. Kenney of Case Western Reserve University for a sample of  $\text{Si}(\text{OSi}(n\text{-hexyl})_3)_2\text{Nc}$ , (SINC).

EVS thanks Prof. T. Boggess for helpful discussions.

## References

1. See for example, a) D.S. Chemla, J. Zyss (eds.): *Nonlinear Optical Properties of Organic Molecules and Crystals*, Vols. 1 and 2 (Academic, Orlando, 1987) b) R.A. Hann, D. Bloor (eds.): *Organic Materials for Nonlinear Optics* (The Royal Society of Chemistry, London, 1989) c) J. Messier, F. Kajzar, P. Prasad, D. Ulrich (eds.): *Nonlinear Optical Effects in Organic Polymers* NATO ASI Series E, Vol. 162 (Kluwer, Dordrecht 1989)
2. M. Sheik-bahae, A.A. Said, E.W. Van Stryland: *Opt. Lett.* **14**, 955–957 (1989)

3. M. Sheik-bahae, A.A. Said, T.H. Wei, D.J. Hagan, E.W. Van Stryland: IEEE J. QE-**26**, 760–769 (1990)
4. Z.Z. Ho, C.Y. Ju, W.M. Hetherington III: J. Appl. Phys. **62**, 716 (1987)
5. M.K. Casstevens, M. Samoc, J. Pflieger, P.N. Prasad: J. Chem. Phys. **92**, 2019 (1990)
6. D.R. Coulter, V.M. Miskowski, J.W. Perry, T.H. Wei, E.W. Van Stryland, D.J. Hagan: *Materials for Optical Switches, Isolators and Limiters*, ed. by M.J. Soileau, Proc. SPIE **1105**, 42–51 (1989)
7. J.W. Wu, J.R. Heflin, R.A. Norwood, K.Y. Wong, O. Zamani-Khamiri, A.F. Garito, P. Kalyanaraman, J.R. Sounik: J. Opt. Soc. Am. B **6**, 707 (1989)
8. J.S. Shirk, J.R. Lindle, F.J. Bartoli, C.A. Hoffman, A.H. Kafafi, A.W. Snow: Appl. Phys. Lett. **55**, 1287 (1989)
9. A.F. Garito, J.R. Heflin, N.Q. Wang, Y.M. Cai: Technical digest of the conference on *Nonlinear Optics: Materials, Phenomena and Devices* (IEEE, Washington D.C. 1990) p. 73
10. A. Kaltbeitzl, D. Neher, C. Bubeck, T. Sauer, G. Wegner, W. Caseri: In *Electronic properties of Conjugated Polymers III*, Springer Series in Solid State Sci. **91**, 220 (1989)
11. J.W. Perry, L.R. Khundkar, D.L. Coulter, D. Alvarez Jr., S.R. Marder, T.H. Wei, M.J. Sence, E.W. Van Stryland, D.J. Hagan: In *Organic Molecules for Nonlinear Optics and Photonics*, ed. by J. Messier, F. Kajzar, P. Prasad, NATO ASI Series E, Vol. 194 (Kluwer, Dordrecht 1991) p. 369
12. M. Gouterman: In *The Porphyrins*, ed. by D. Dolphin (Academic, New York 1978) Vol. III, p. 1
13. F. Gires, F. Combaud: J. de Phys. **26**, 325 (1965)
14. J.A. Armstrong: J. Appl. Phys. **36**, 471 (1965)
15. M. Hercher, W. Chu, D.L. Stockman: IEEE J. QE-**4**, 954 (1968)
16. T. Ohno, S. Kato, A. Yamada, T. Tanno: J. Phys. Chem. **87**, 775 (1983)
17. W. Blau, H. Byrne, W.M. Dennis, J.M. Kelly: Opt. Commun. **56**, 25 (1985)
18. B.L. Wheeler, G. Nagasubramanian, A.J. Bard, L.A. Schectman, D.R. Dininny, M.E. Kenney: J. Am. Chem. Soc. **106**, 7404 (1984)
19. J.H. Brannon, D. Magde: J. Am. Chem. Soc. **102**, 62 (1980)
20. D.C. Hutchings, M. Sheik-Bahae, D.J. Hagan, E.W. Van Stryland: Opt. Quantum Electron (to be published, 1991)